rather than by its polarity. The influence of the solvent basicity is reduced when the substituent R becomes more bulky. Because of the basic properties of water, these results imply that a hydrophobic environment and protection from solvent attack are indeed essential factors for the stabilization of the $[4Fe-4S]^{3+}$ core in HP proteins. Another conclusion may be that a low-molecular-weight thiolate cluster compound when dissolved in a low-donor-number solvent like NB or DC can be regarded to be a good model system for the active site of HP proteins.

Acknowledgment. We thank A. M. Roelofsen for the recording of the cyclic voltammograms in benzonitrile. This investigation was supported by the Netherlands Foundation for Chemical Research (SON), with financial aid from the Netherlands Organization for Scientific Research (NWO), and by the Centre National de la Recherche Scientifique-DRCI.

Registry No. AN, 75-05-8; BN, 100-47-0; ACN, 67-64-1; DC, 75-09-2; DMF, 68-12-2; NB, 98-95-3; THF, 109-99-9; DMSO, 67-68-5; $[Fe_4S_4(SPh)_4]^{2-}$, 52325-39-0; $[Fe_4S_4(S\text{-}t\text{-}Bu)_4]^{2-}$, 51913-87-2; $[Fe_4S_4(SEt)_4]^{2-}$, 52261-51-5; $[Fe_4S_4(S\text{-}n\text{-}Pr)_4]^{2-}$, 52325-40-3; $[Fe_4S_4(SCH_2Ph)_4]^{2-}$, 52349-82-3; $[Fe_4S_4(S\text{-}p\text{-}C_6H_4Cl)_4]^{2-}$, 55787-38-7; $[Fe_4S_4(S\text{-}p\text{-}C_6H_4CH_3)_4]^{2-}$, 51899-68-4; $[Fe_4S_4(SCH_2CH_2OH)_4]^{2-}$, 62851-99-4; $[Fe_4S_4(SPh)_4]^-$, 97365-72-5; $[Fe_4S_4(S\text{-}t\text{-}Bu)_4]^-$, 126752-32-7; $[Fe_4S_4(SEt)_4]^-$, 134566-32-8; $[Fe_4S_4(S\text{-}n\text{-}Pr)_4]^-$, 134566-33-9; $[Fe_4S_4(SCH_2Ph)_4]^-$, 134593-43-4; $[Fe_4S_4(S\text{-}p\text{-}C_6H_4Cl)_4]^-$, 134566-34-0; $[Fe_4S_4(S\text{-}p\text{-}C_6H_4CH_3)_4]^-$, 134566-35-1; $[Fe_4S_4(SCH_2CH_2OH)_4]^-$, 134566-36-2; Pt, 7440-06-4; $[Fe_4S_4(SPh)_4]^{3-}$, 52627-89-1; $[Fe_4S_4(S\text{-}t\text{-}Bu)_4]^{3-}$, 91294-54-1; $[Fe_4S_4(SCH_2CH_2OH)_4]^{3-}$, 134566-37-3; $[Fe_4S_4(S\text{-}p\text{-}C_6H_4CH_3)_4]^{3-}$, 67724-72-5; $[Fe_4S_4(SCH_2C_6H_5)_4]^{3-}$, 63138-11-4; $[Fe_4S_4(SEt)_4]^{3-}$, 52499-30-6; $[Fe_4S_4(SPh)_4]$, 134566-38-4; $[Fe_4S_4(S\text{-}t\text{-}Bu)_4]$, 134566-39-5.

(25) Kadish, K. M.; Das, K.; Schaeper, D.; Merrill, C. L.; Welch, B. R.; Wilson, L. J. *Inorg. Chem.* **1980**, *19*, 2816.

Contribution from the Ottawa-Carleton Chemistry Institute, Carleton University, Ottawa, Canada K1S 5B6, Chemistry Division, National Research Council of Canada, Ottawa, Canada K1A 0R6, and Institute for Materials Research, McMaster University, Hamilton, Ontario, Canada L8S 4M1

Long-Range Antiferromagnetic Coupling between Two Ruthenium(III) Ions Bridged by a 1,4-Dicyanamidobenzene Dianion Ligand

Manuel A. S. Aquino,[†] Florence L. Lee,[‡] Eric J. Gabe,[‡] J. E. Greedan,[§] and Robert J. Crutchley*,[†]

Received July 24, 1990

The study of polymetallic complexes in which coupling between metals is propagated via a bridging molecule has clear application to the design of novel magnetic and electronic solid-state materials and to the role of polymetallic sites in biological processes.[1,2] A fundamental property to be understood is the distance dependence of metal–metal interactions. Researchers[3] have proposed the relation

$$|2J_{\text{lim}}| = 1.35 \times 10^7 \exp(-1.80R) \qquad (1)$$

for the limiting value of J (cm^{-1}),[4] the magnetic exchange coupling constant, and R (Å), the distance between metal ions. In approximate agreement with eq 1, a study of the distance dependence of the magnetic coupling between two Cu(II) complexes bridged by 4,4'-bipyridine (metal ions separated by 11.1 Å) found $2J$ = −0.9 cm^{-1}.[5] The authors pointed out that at this magnitude of coupling it would be difficult to distinguish between intermolecular and intramolecular mechanisms. In contrast, a later study found moderately strong intramolecular antiferromagnetic coupling ($2J$ = −140 cm^{-1}) between Cu(II) ions separated by 11.25 Å in $[X_2Cu_2(OH_2)(\mu\text{-terephthalato})][ClO_4]_2$, where X = 1,4,7-trimethyl-1,4,7-triazacyclononane.[6] The difference in magnetic coupling between these two results is clearly dependent on the nature of the interaction of the magnetic orbitals with the bridging ligand. For maximum resonance exchange of the magnetic orbitals,[1,7] the bridging ligand should possess a HOMO delocalized on its donor atoms with the correct symmetry and energy to optimize its interaction with the magnetic orbitals. Even if the bridging ligand's HOMO has improper symmetry to interact with the magnetic orbitals, the spin polarization mechanism can still induce antiferromagnetic coupling.[1,8]

[†] Carleton University.
[‡] National Research Council of Canada.
[§] McMaster University.

Table I. Crystal Data for the Tetraphenylarsonium Salt of the 1,4-Dicyanamido-2,3,5,6-tetramethylbenzene Dianion ($[AsPh_4]_2[L]$)

formula	$As_2N_4C_{60}H_{52}$	MW	966.84
space group	$P2_1/n$	Z	2
cryst syst	monoclinic	D_c; g/cm^3	1.323
a, Å	12.6115 (24)	temp, °C	22
b, Å	14.3029 (17)	radiation (λ, Å)	Mo (0.709 30)
c, Å	13.6986 (14)	R factor[a]	0.051
β, deg	100.820 (10)	R_w factor[b]	0.051
V, Å^3	2427.0 (6)		

[a] $R = \sum||F_o| - |F_c||/\sum|F_o|$. [b] $R_w = (\sum w(|F_o| - |F_c|)^2/\sum w|F_o|^2)^{1/2}$.

The possibility that long-range antiferromagnetic coupling might occur between magnetic orbitals bridged by an easily oxidized, extended π HOMO system led us to prepare the dinuclear complex $[\mu\text{-L}\{(NH_3)_5Ru\}_2][ClO_4]_4$ (**1**), where L^{2-} = 1,4-dicyanamido-2,3,5,6-tetramethylbenzene dianion. The physical characterization of this complex, including its temperature-dependent magnetic properties, is the subject of this report.

Experimental Section

Physical Measurements. The equipment used to perform cyclic voltammetry and UV–vis spectroscopy has been described in a previous paper.[9] Temperature-dependent magnetic measurements were performed on a Quantum Design SQUID magnetometer from 5 to 300 K in a 1.0-T field. Elemental analyses were performed by Canadian Microanalytical Services Ltd.

Materials. All solvents and solid chemicals were reagent grade or better. $[(NH_3)_5Ru(OH_2)][PF_6]_2$ was prepared by literature methods.[10] Protonated 1,4-dicyanamido-2,3,5,6-tetramethylbenzene was prepared from its thiourea precursor.[9,11]

Preparation of Bis(tetraphenylarsonium) 1,4-Dicyanamido-2,3,5,6-tetramethylbenzene(2−) ($[AsPh_4]_2[L]$). The protonated ligand LH_2 (0.68 g) and NaOH (3 g) were placed in a 100-mL round-bottom flask and purged with argon. A previously degassed 30-mL aliquot of water was transferred to the reaction flask under argon. The mixture was stirred until complete dissolution. Tetraphenylarsonium chloride monohydrate (2.6 g) was dissolved into 30 mL of 2.5 M NaOH aqueous solution. This solution was degassed and then transferred under argon to the basic solution of the ligand. The resulting yellow precipitate was filtered out,

(1) Willet, R. D., Gatteschi, D., Kahn, O., Eds. *Magneto-Structural Correlations in Exchanged Coupled Systems*; Reidel: Dordrecht, Holland, 1985.
(2) Marcus, R. A.; Sutin, N. *Biochem. Biophys. Acta* **1985**, *811*, 265.
(3) Coffman, R. E.; Buettner, G. R. *J. Phys. Chem.* **1979**, *83*, 2387.
(4) Here the magnetic interaction between spins S_a and S_b for atoms A and B is of the form $H = -2JS_aS_b$.
(5) Julve, M.; Verdaguer, M.; Faus, J.; Tinti, F.; Moratal, J.; Monge, A.; Gutierrez-Puebla, E. *Inorg. Chem.* **1987**, *26*, 3520.
(6) Chaudhuri, P.; Oder, K.; Wieghardt, K.; Gehring, S.; Haase, W.; Nuber, B.; Weiss, J. *J. Am. Chem. Soc.* **1988**, *110*, 3657.
(7) Tinti, F.; Verdaguer, M.; Kahn, O.; Savariault, J.-M. *Inorg. Chem.* **1987**, *26*, 2380.
(8) Rosen, R. K.; Anderson, R. A.; Edelstein, N. M. *J. Am. Chem. Soc.* **1990**, *111*, 4588.
(9) Crutchley, R. J.; Naklicki, M. L. *Inorg. Chem.* **1989**, *28*, 1955.
(10) Callahan, R. W.; Brown, G. M.; Meyer, T. J. *Inorg. Chem.* **1975**, *14*, 1443.
(11) Aumuller, A.; Hunig, S. *Liebigs Ann. Chem.* **1986**, 142.

0020-1669/91/1330-3234$02.50/0

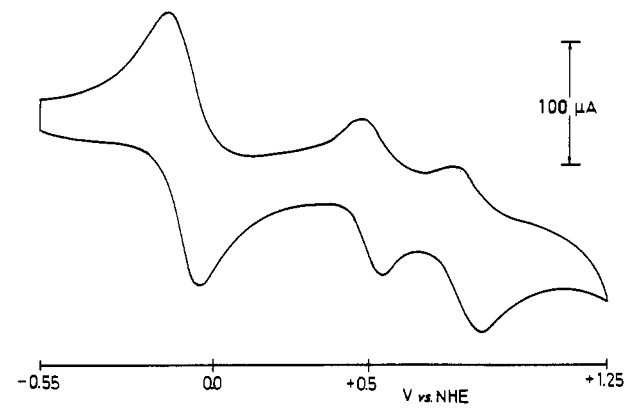

Figure 1. Cyclic voltammogram of **1** in 0.1 M NaCl aqueous solution taken with a glassy-carbon working electrode. Scan rate = 100 mV s^{-1}.

washed with ice cold water, and then vacuum dried. The final product was air sensitive and hygroscopic. Yield: 2.1 g (68%).

Preparation of [μ-L{$(NH_3)_5Ru$}$_2$][ClO_4]$_4$ (1). Under argon, in 80 mL of acetone, 0.49 g (0.5 mmol) of $[AsPh_4]_2[L]$ and 0.54 g (1.2 mmol) of $[(NH_3)_5Ru(OH_2)][PF_6]_2$ were permitted to react for 2 h. After air oxidation and filtration, the crude product was isolated as a bromide salt by the addition of 2.42 g (7.5 mmol) of tetrabutylammonium bromide and then purified by ion-exchange chromatography by using Sephadex C25-120 resin and eluting with 1 M NaCl solution. The dinuclear complex was precipitated from the eluent by the addition of $NaClO_4$ and then recrystallized by ether diffusion into an acetone solution, affording dark green-blue crystals of complex **1**, $[\mu\text{-L}\{(NH_3)_5Ru\}_2][ClO_4]_4\cdot{}^2/_3CH_3COCH_3$. Yield: 78 mg (11%). The presence of acetone in the product was verified by IR spectroscopy. Anal. Calcd for $C_{14}H_{46}N_{14}O_{16.66}Cl_4Ru_2$: C, 16.47; H, 4.53; N, 19.21. Found: C, 16.75; H, 4.36; N, 19.61.

X-ray Diffraction Studies. A summary of crystal data for $[AsPh_4]_2[L]$ is given in Table I. Deep yellow crystals of the dianion ligand were grown by allowing a concentrated warm dimethyl sulfoxide solution to cool to room temperature. The diffraction intensities were collected on a Nonius diffractometer with Mo Kα radiation by using the $\theta/2\theta$ scan technique with profile analysis.[12] Unit cell parameters were obtained by least-squares refinement of the setting angle for 22 reflections ($40 < 2\theta < 45$). Lorentz and polarization factors were applied, but no corrections were made for absorption.

The structures were solved by direct methods and refined by full-matrix least squares. Hydrogen atom positions were calculated. All the calculations were performed with the NRCVAX Crystal Structure Package.[13] The atomic parameters, anisotropic thermal parameters, final structure factors, and complete bond lengths and bond angles are available as supplementary material.

Results and Discussion

The UV-vis spectra of mononuclear pentaammineruthenium(III) complexes of phenylcyanamide anion ligands have been investigated, and assignments have been made to the major features.[9,14] In these complexes, intense $\pi-\pi^*$ transitions are found in the UV region and two LMCT bands are found in the visible region. The LMCT bands arise out of the π interaction between Ru(III) and the two lone electron pairs of π symmetry on the cyanamide anion group. The dinuclear ruthenium(III) complexes of 1,4-dicyanamidobenzene dianion ligands are expected to have the same basic features as their mononuclear analogues. In this regard, the major bands found in the absorption spectrum of complex **1** are intense phenyl ring $\pi-\pi^*$ bands at 213 (38000), 252 (14450), and 353 nm (3160 M^{-1} cm^{-1}) and two ligand to metal charge-transfer bands at 465 (3160) and 795 nm (8130 M^{-1} cm^{-1}).

The cyclic voltammogram of free L^{2-} in acetonitrile solution[15] shows two reversible one-electron waves at -0.565 and -0.070 V vs NHE, corresponding to the L(-/2-) and L(0/-) couples, respectively. The cyclic voltammogram of **1** is shown in Figure 1.[16] In previous studies of mononuclear pentaammineruthenium(III) phenylcyanamide complexes,[9,14] the Ru(III/II) couple was determined to range from approximately 0 to -0.3 V vs NHE, depending on the nature of the anionic phenylcyanamide ligand. It therefore seems likely that the large wave centered at -0.083 V in Figure 1 corresponds to the Ru(III/II) couple. The two smaller waves at 0.475 and 0.822 V correspond to the one-electron ligand redox couples, anodically shifted from their free ligand values because of the π interaction between the Ru(III) ions and the cyanamide bridging ligand.[9] The peak current for the Ru(III/II) redox wave is approximately twice as large as that for the one-electron ligand redox waves. In addition, the anodic and cathodic wave separation ($E_{pc} - E_{pa}$ = 72 mV) of the Ru(III/II) couple is greater than that seen for the mononuclear pentaammineruthenium(III) complexes (60-65 mV at a scan rate of 100 mV s^{-1}).[14] Similar peak shapes in weak *electronically* coupled dipyridyl-bridged bis(pentaammineruthenium) complexes[17] are the result of two successive one-electron processes being so close in proximity that only a single wave can be resolved.

The probable structure of **1** can be derived by using information from the crystal structures of $[(NH_3)_5Ru(2,3\text{-dichlorophenylcyanamido})][SO_4]$[14] and free L^{2-}. The crystal structure of the mononuclear Ru(III) complex showed that the Ru(III) ion binds to the cyano nitrogen of the cyanamide group with a bond angle of 171°.[14] Crystal data and atomic positional parameters for significant atoms of $[AsPh_4]_2[L]$ are given in Tables I and II, respectively, and Figure 2 illustrates the structure of L^{2-} with important bond lengths and angles included in the figure caption. The structure of L^{2-} reveals that the approximately linear cyanamide anion groups are in an anti configuration and clearly out of the phenyl ring plane. It is not unreasonable to suggest that **1** would adopt the most stable conformation of the bridging ligand in the solid state.[18] The through-space distance between Ru(III)

Table II. Significant Atomic Parameters[a] and B_{iso}[b] Values for $[AsPh_4]_2[L]$

	x	y	z	B_{iso}[c]
N1	0.5471 (6)	0.4492 (4)	0.3157 (6)	4.9 (4)
N2	0.5952 (6)	0.5569 (5)	0.1903 (6)	6.1 (4)
C1	0.5983 (7)	0.5327 (5)	0.4743 (6)	4.0 (4)
C2	0.5238 (7)	0.4770 (5)	0.4079 (6)	3.9 (4)
C3	0.4283 (6)	0.4440 (5)	0.4337 (6)	3.7 (4)
C4	0.7062 (6)	0.5625 (6)	0.4483 (6)	5.2 (5)
C5	0.5725 (7)	0.5082 (7)	0.2534 (7)	4.3 (5)
C6	0.3520 (6)	0.3826 (5)	0.3582 (5)	4.6 (4)

[a] The atom number scheme is given in Figure 2. [b] Estimated standard deviations are in parentheses. [c] B_{iso} is the mean of the principal axes of the thermal ellipsoid in Å^2.

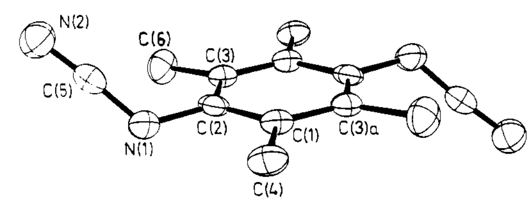

Figure 2. ORTEP drawing of the dianion ligand, L^{2-}. Selected bond lengths (Å) and bond angles (deg): N2-C5, 1.187 (14); C5-N1, 1.283 (14); N1-C2, 1.410 (11); C2-C1, 1.416 (12); C1-C3$_a$, 1.405 (12); C1-C4, 1.531 (12); C2-C3, 1.403 (12); C3-C6, 1.547 (10); N2-C5-N1, 174.6 (9); C5-N1-C2, 121.6 (7); N1-C2-C1, 120.8 (8); C2-C1-C3$_a$, 117.8 (8); C2-C3-C1$_a$, 120.4 (7).

(12) Grant, D. F.; Gabe, E. J. *J. Appl. Crystallogr.* **1978**, *11*, 114.
(13) Gabe, E. J.; Lee, F. L.; Lepage, Y. *J. Appl. Crystallogr.* **1989**, *22*, 384.
(14) Crutchley, R. J.; McCaw, K.; Lee, F. L.; Gabe, E. J. *Inorg. Chem.* **1990**, *29*, 2576.

(15) Cyclic voltammetry of $[AsPh_4]_2[L]$ was performed in acetonitrile with 0.1 M tetrabutylammonium hexafluorophosphate electrolyte and with a platinum working electrode at 25 °C and at a scan rate of 100 mV s^{-1}.
(16) Cyclic voltammetry of **1** was performed in aqueous solution with 0.1 M NaCl and with a glassy-carbon working electrode at 25 °C and at a scan rate of 100 mV s^{-1}.

(17) Sutton, J. E.; Sutton, P. M.; Taube, H. *Inorg. Chem.* **1979**, *18*, 1017. Kim, Y.; Lieber, C. M. *Ibid.* **1989**, *28*, 3990.

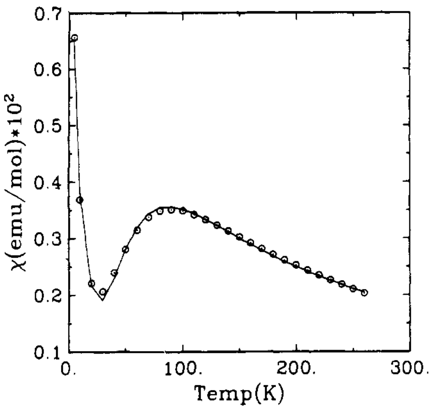

Figure 3. Molar magnetic susceptibility from 5 to 300 K in a 1.0-T field for **1**. The solid line is a fit to eq 2 plus a Curie–Weiss term, which yields the parameters given in the text.

ions is then estimated to be 13 Å.

Temperature-dependent magnetic susceptibility data for **1** are plotted in Figure 3 and show a broad maximum at about 90 K. This feature is characteristic of intramolecular antiferromagnetic exchange. Intermolecular antiferromagnetic couplings normally result in a phase transition to a long-range ordered state, which gives a sharp maximum at the transition temperature (Neel temperature). Intermolecular exchange has been studied in monomeric Ru(III) complexes with similar ligands, and the effect occurs at much lower temperatures than those observed here.[19a]

The simplest model for analysis of $S = {}^1/_2$, spin-coupled dimers is the so-called Bleaney–Bowers expression:[19b]

$$\chi_m = (2N\bar{g}^2\beta^2/3kT)[1 - {}^1/_3\exp(-2J/kT)]^{-1} \qquad (2)$$

Here J is the exchange coupling constant, $\bar{g}$ is the powder-averaged g value, and β is the Bohr magneton. This model neglects orbital angular momentum contributions, which are important for Ru(III), $t_{2g}{}^5$. Drillon et al.[20] have developed procedures for including the orbital contribution for $t_{2g}{}^n$ configurations, but analytical expressions are not available. Nonetheless, the use of eq 2 should provide a good first approximation for J. Thus, the data of Figure 3 were analyzed by using eq 2 and included a Curie–Weiss term, $\chi = C/(T - \Theta)$, to model the sharp upturn seen at low temperatures ascribed to a paramagnetic impurity. The fit, the solid line in Figure 3, is excellent, yielding the parameters $J/k = -77$ K, $\bar{g} = 1.76$,[21] $C = 0.047$ emu cm^{-3} K^{-1}, and $\Theta = -2.2$ K.

It is interesting to contrast the antiferromagnetic behavior found in complex **1** with the absence of significant magnetic interactions ($|J| < 0.2$ cm^{-1}) found in dinuclear ruthenium(III) complexes bridged by pyrazine,[22] 4,4′-bipyridine,[23] and *trans*-1,2-bis(4-pyridyl)ethylene.[23] It is probable that the high-energy HOMO of L^{2-} in complex **1** provides a pathway for magnetic interaction that is energetically unavailable to the above complexes.

An extended Huckel calculation[24] of the free L^{2-} ligand resulted in the following schematized drawing of its HOMO:

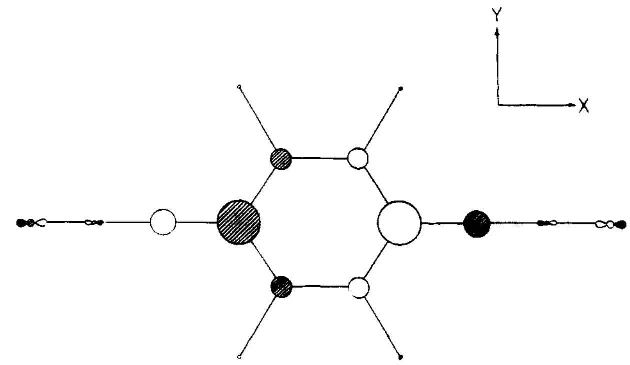

The 2p orbital contributions are indicated where lobe size is drawn in proportion to the relative contribution of that atomic orbital to the HOMO. Minor atomic orbital contributions are omitted for clarity. It is important to note that the HOMO spans the bridging ligand and can directly interact with the magnetic orbital of each ruthenium(III) ion. Intramolecular magnetic coupling via this HOMO could occur by resonance-exchange and/or spin-polarization mechanisms.[1,19] Future studies of dinuclear complexes in which the extent of magnetic coupling between Ru(III) ions can be varied depending on the nature of the 1,4-dicyanamidobenzene dianion bridging ligand should reveal the dominant mechanism and together with crystal structures of the complexes provide the experimental background necessary for a quantitative theoretical description.

Acknowledgment. This work was funded by the NSERC (Canada) in the form of an operating grant and University Research Fellowship to R.J.C. and a Postgraduate Scholarship to M.A.S.A. We thank C. V. Stager for the use of a Quantum Design SQUID magnetometer and J. N. Reimers for his assistance with the data analysis. We also thank Johnson Matthey, Inc., for their loan of ruthenium trichloride hydrate.

Registry No. $1\cdot(ClO_4)_4\cdot{}^2/_3CH_3COCH_3$, 134627-11-5; 1^{2+}, 134627-12-6; L^-, 134594-78-8; L, 98507-16-5; L^{2-}, 134594-74-4; $[AsPh_4]_2[L]$, 134594-75-5; $[(NH_3)_5Ru(OH_2)][PF_6]_2$, 34843-18-0; tetraphenylarsonium 2,5-dichloro-1,4-dicyanamidobenzene(2−), 134594-76-6; tetraphenylarsonium 2,3,5,6-tetrachloro-1,4-dicyanamidobenzene(2−), 129239-19-6; tetraphenylarsonium 1,4-dicyanamidobenzene(2−), 134594-77-7.

Supplementary Material Available: Full listings of crystal structure data, atomic parameters, anisotropic thermal parameters, bond lengths, and bond angles (5 pages); a listing of final structure factors (16 pages). Ordering information is given on any current masthead page.

(18) We have obtained crystal structures of the tetraphenylarsonium salts of the following dianion ligands: 2,5-dichloro-1,4-dicyanamidobenzene, 2,3,5,6-tetrachloro-1,4-dicyanamidobenzene, and unsubstituted 1,4-dicyanamidobenzene. In all structures, each cyanamide group is nearly coplanar with the phenyl ring and in a trans configuration. For L^{2-}, it would seem that the weaker π interaction between a cyanamide group and the phenyl ring together with the steric hinderance of ortho-methyl groups is enough to cause the cyanamide groups to move out of plane while still maintaining a trans configuration.

(19) Carlin, R. L. *Magnetochemistry*; Springer-Verlag: Berlin, 1986: (a) p 230; (b) p 75.

(20) Drillon, M.; Georges, R. *Phys. Rev. B* **1981**, *24*, 1278.

(21) This value of $\bar{g}$ should be treated with caution. In our data analysis, the main effect of the impurity will be to reduce the value of $\bar{g}$ artificially.

(22) Bunker, B. C.; Drago, R. S.; Hendrickson, D. N.; Richman, R. M.; Kessell, S. L. *J. Am. Chem. Soc.* **1978**, *100*, 3805.

(23) Johnson, E. C.; Callahan, R. W.; Eckberg, R. P.; Hatfield, W. E.; Meyer, T. J. *Inorg. Chem.* **1979**, *18*, 618.

(24) The extended Huckel calculation was performed with the Quantum Chemistry Program Exchange Program No. QCMP 011, FORTICON 8, for personal computers.

Contribution from the Department of Chemistry, Faculty of Science, Okayama University, Tsushima, Okayama 700, Japan

Stereochemistry of Six-Coordinated Silicon Complexes. 1. Stereoselectivity and CD Spectra of Tris(optically active β-diketonato)silicon(IV) Complexes

Takashi Shimizutani and Yuzo Yoshikawa*

Received September 21, 1990

Introduction

There have been very few studies about six-coordinated silicon(IV) complexes compared to four-coordinated ones. Six-coordinated complexes of phthalocyaninate,[1] octaethylporphinate,[2] heterocyclic amines,[3] *N,N*-dimethylformamide,[4] and Schiff bases[5]

(1) Joyner, R. D.; Cekad, J., Jr.; Kenney, M. E. *J. Inorg. Nucl. Chem.* **1960**, *15*, 387.

(2) Buchler, J. W.; Puppe, L.; Rohback, K.; Schneehage, H. H. *Chem. Ber.* **1973**, *106*, 2710.

